frontiers | Frontiers in Immunology

TYPE Brief Research Report
PUBLISHED 15 November 2023
DOI 10.3389/fimmu.2023.1293766

OPEN ACCESS

EDITED BY
Laura Vesala,
Tampere University, Finland

REVIEWED BY
Ilias Kounatidis,
The Open University, United Kingdom
Holly Stephenson,
University of Plymouth, United Kingdom

*CORRESPONDENCE
Angela Giangrande
angela@igbmc.fr
Pierre B. Cattenoz
cattenoz@igbmc.fr

RECEIVED 13 September 2023
ACCEPTED 26 October 2023
PUBLISHED 15 November 2023

CITATION
Bazzi W, Monticelli S, Delaporte C, Riet C, Giangrande A and Cattenoz PB (2023) Gcm counteracts Toll-induced inflammation and impacts hemocyte number through cholinergic signaling. *Front. Immunol.* 14:1293766. doi: 10.3389/fimmu.2023.1293766

Gcm counteracts Toll-induced inflammation and impacts hemocyte number through cholinergic signaling

Wael Bazzi[1,2,3,4], Sara Monticelli[1,2,3,4], Claude Delaporte[1,2,3,4], Céline Riet[1,2,3,4], Angela Giangrande[1,2,3,4]* and Pierre B. Cattenoz[1,2,3,4]*

[1]Université de Strasbourg, IGBMC UMR 7104- UMR-S 1258, Illkirch, France, [2]CNRS, UMR 7104, Illkirch, France, [3]Inserm, UMR-S 1258, Illkirch, France, [4]IGBMC, Institut de Génétique et de Biologie Moléculaire et Cellulaire, Illkirch, France

Hemocytes, the myeloid-like immune cells of *Drosophila*, fulfill a variety of functions that are not completely understood, ranging from phagocytosis to transduction of inflammatory signals. We here show that downregulating the hemocyte-specific Glial cell deficient/Glial cell missing (Glide/Gcm) transcription factor enhances the inflammatory response to the constitutive activation of the Toll pathway. This correlates with lower levels of glutathione S-transferase, suggesting an implication of Glide/Gcm in reactive oxygen species (ROS) signaling and calling for a widespread anti-inflammatory potential of Glide/Gcm. In addition, our data reveal the expression of acetylcholine receptors in hemocytes and that Toll activation affects their expressions, disclosing a novel aspect of the inflammatory response mediated by neurotransmitters. Finally, we provide evidence for acetylcholine receptor nicotinic acetylcholine receptor alpha 6 (nAchRalpha6) regulating hemocyte proliferation in a cell autonomous fashion and for non-cell autonomous cholinergic signaling regulating the number of hemocytes. Altogether, this study provides new insights on the molecular pathways involved in the inflammatory response.

KEYWORDS

hemocytes, toll, Glide/Gcm, nAchRalpha6, inflammation, *Drosophila*

Introduction

Inflammation is the first response of the organism to pathogenic cues and tissue damages. It allows the removal of the infectious agent and induces the healing process. Prolonged or chronic activation of the inflammatory response is highly detrimental for the organism and constitutes a major aggravating factor in the etiology of many diseases ranging from cancers to neurodegenerative disorders (1–3). Thus, the coordination of the

inflammatory response requires robust regulatory mechanisms to prevent its adverse effects.

The inflammatory response is well conserved across evolution, and the *Drosophila* model has been instrumental for the identification of the molecular mechanisms underlying innate immunity (4). Two major signaling pathways transducing the inflammatory response are the Toll and the Janus kinase/signal transducer and activator of transcription (Jak/Stat) pathways. Microbial particles activate the Toll receptor, which promotes the degradation of the nuclear factor-kappa B (NF-κB) inhibitor Cactus (i.e., Inhibitor-kappa B (IκB) in mammals), hence allowing the nuclear translocation of the NF-κB transcription factors Dorsal (Dl) and Dorsal-related immunity factor (Dif) and the transcription of effector genes (5, 6). The Jak/Stat pathway is activated in response to cytokine signaling. Following the neutralization of the pathogen, the restoration of homeostasis requires the inhibition of the inflammatory pathways, which depends on potent negative autoregulatory loops where each pathway activates its own inhibitors (7, 8).

Drosophila hemocytes are myeloid-like cells that respond to inflammatory challenges. Like in vertebrates, they are produced by two hematopoietic waves occurring in different anlagens and times. The first-wave hemocytes originate from the procephalic mesoderm of the embryo and circulate in the larval hemolymph or reside between the muscles and the cuticle (i.e., sessile pockets, dorsal stripes) (Figure 1A) (10, 11). The second wave occurs in the larval lymph gland, which histolyzes and releases a second pool of hemocytes after puparium formation (or already in the larva, upon immune challenge) (10). The Toll and the Jak/Stat pathways activate the hemocytes originating from the two hematopoietic waves, leading to their differentiation into lamellocytes, large cells that encapsulate pathogens too big to be phagocytosed (12, 13).

The transcription factor Glial cell deficient/Glial cell missing (Glide/Gcm, Gcm throughout the article) is specifically expressed in the hemocytes of the first wave and has an anti-inflammatory role that is conserved in evolution (13, 14). Gcm inhibits the pathway by activating Jak/Stat inhibitors (13), raising the question of whether this transcription factor has a general role in the inflammatory response. We here demonstrate that Gcm impacts the Toll pathway. Animals displaying constitutive Toll pathway activation and sensitized hemocytes due to Gcm downregulation produce more lamellocytes than control hemocytes. Transcriptomic analyses reveal that such hemocytes express lower levels of glutathione S-transferase (Gst) and produce higher levels of reactive oxygen species (ROS), which may explain their higher propensity to produce lamellocytes. In addition, our data highlight the expression of several neurotransmitter receptors in these sensitized hemocytes, and we show that these receptors regulate the number of hemocytes in the larva.

In sum, the present work indicates that Gcm acts as a general anti-inflammatory transcription factor inhibiting the Toll pro-inflammatory pathway. Moreover, it highlights a new signaling channel through which neurotransmitters from the nervous system modulate the immune system during inflammation.

Materials and methods

Fly strains and genetics

Drosophila stocks and crosses were maintained on standard fly medium (75 g/L organic corn flour, 7.5 g/L soybean flour, 15 g/L dry yeast, 15 g/L sucrose, 5.5 g/L agar, 5 mL/L propionic acid) at 25°C under 60% humidity with a day/light cycle of 12 h/12 h. The stocks used are detailed in the Supplementary Methods.

Monitoring the tumors and hemocyte phenotypes

The tumor and hemocyte and lymph gland phenotypes were scored as in Bazzi et al. (13). Detailed protocols are available in the Supplementary Methods for the estimation of the penetrance of the melanotic tumors, the hemocyte counting, and the lymph gland immunolabeling.

Stranded RNA sequencing on hemocytes from WL3 larvae

The sample preparation and analysis are detailed in the Supplementary Methods. The RNA sequencing (RNA-seq) data have been deposited in the ArrayExpress database at EMBL-EBI (www.ebi.ac.uk/arrayexpress) under accession number E-MTAB-11970.

RNA extraction and qPCR

For the qPCR validation of the transcriptomic data, 20 WL3 of the indicated genotypes were bled on ice-cold Phosphate Buffered Saline (PBS). The cells were then centrifuged at 1,200 rpm at 4°C, and RNA isolation was performed with TRI Reagent (Sigma) following the manufacturer's protocol. The DNase treatment was done with the TURBO DNA-free kit (Invitrogen) and the reverse transcription (RT) with the SuperScript IV (Invitrogen) using random primers. The qPCR assays were done with FastStart Essential DNA Green Master (Roche) with the primers listed in the Supplementary Methods.

The expression levels were calculated relative to the two housekeeping genes *Rp49* and *Act5C* levels using the ΔCt formula: $2\text{^}(\text{average}(Ct_{Rp49}, Ct_{Act5c}) - Ct_{target})$. Triplicates were done for each genotype, and the levels were compared using bilateral Student's t-test after variance analysis.

DHE, pH3, and Dcp-1 quantification

ROS levels were estimated using dihydroethidium (DHE; Sigma) (15). The DHE intensity averages were compared using bilateral Student's t-test. For the estimation of the number of

10.3389/fimmu.2023.1293766

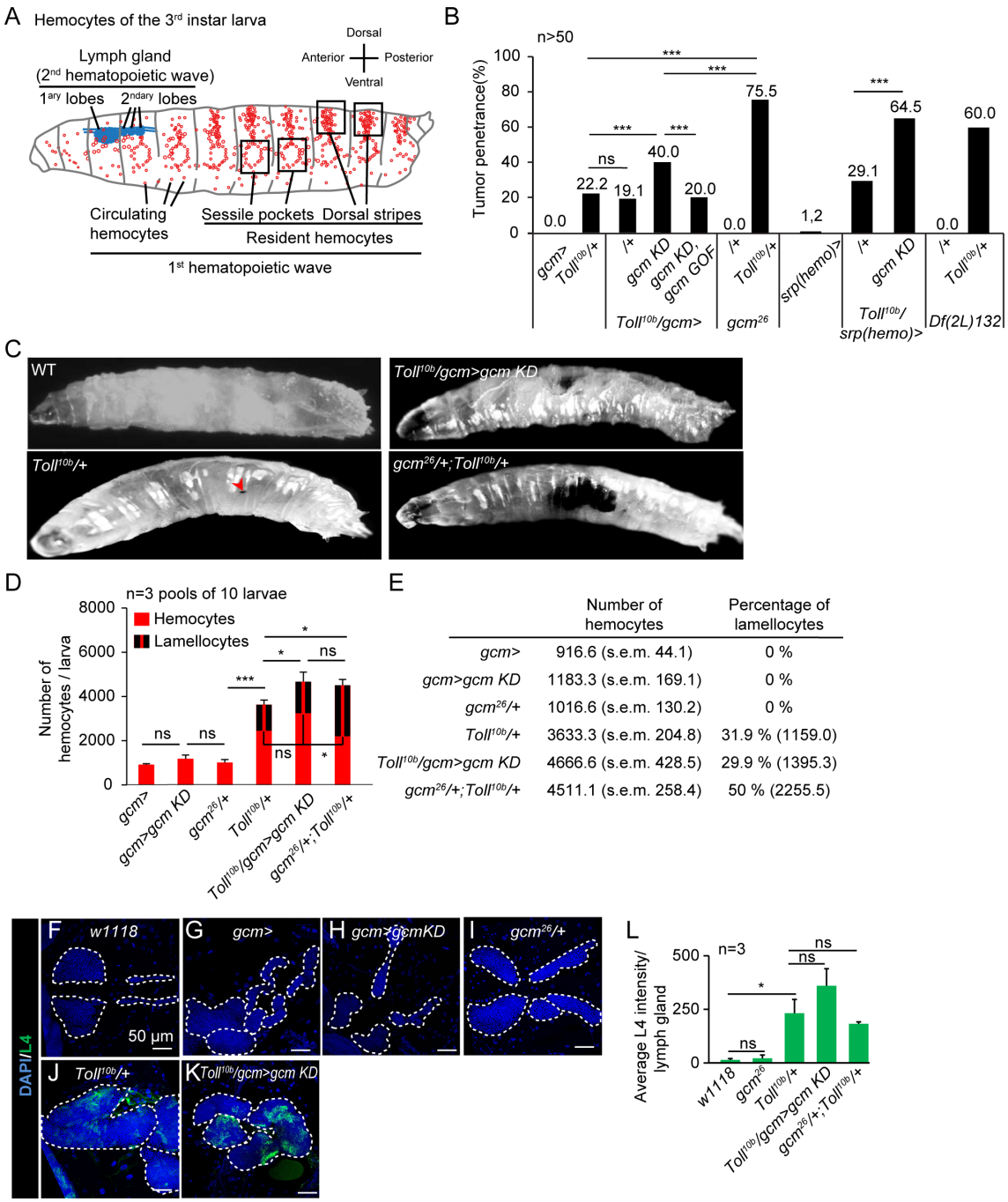

FIGURE 1
Sensitized hemocytes enhance the inflammatory response induced by Toll activation. **(A)** Schematic representation of the hemocytes of the *Drosophila* wandering L3 (WL3). The orientation of the larva is indicated on the right. The larva is mostly populated by hemocytes originating from the first hematopoietic wave during embryogenesis. In the larva, the embryonic hemocytes (in red) are circulating in the hemolymph or become resident and aggregate between the muscles and the cuticle, laterally around the oenocytes to form the sessile pockets or dorsally to form the dorsal stripes. A second hematopoietic wave is taking place at the larval stage in the lymph gland (in blue), composed of successive lobes arranged along the cardiac tube, which produce hemocytes that are released shortly after puparium formation during metamorphosis (9). **(B)** Penetrance of melanotic tumors (n > 50) in WL3 of the indicated genotype. The p-values were estimated with a chi-square test for frequency comparison. **(C)** WL3 of the indicated genotypes. The red arrowhead indicates a small melanotic tumor. **(D, E)** Total number of hemocytes and lamellocyte contribution (n = 3, using 10 larvae/replicate). The p-values were estimated by ANOVA followed by Student's *post-hoc* test. **(F–K)** Lymph glands from WL3 of the following genotypes: *w1118* **(F)**, *gcmGal4* (*gcm>*, **(G)**, *gcmGal4;UAS-gcmRNAi/+* (*gcm>gcm KD*, **(H)**, gcm^{26}*/+* **(I)**, $Toll^{10b}$*/+* **(J)**, and *gcmGal4/+;UAS-gcmRNAi/*$Toll^{10b}$ ($Toll^{10b}$*/gcm>gcm KD*, **(K)**. The lamellocytes are labeled with an antibody anti-L4 (in green) and the nuclei are labeled with DAPI (in blue). The scale bars represent 50 µm. The white dashed lines highlight the lobes of the lymph glands. **(L)** Quantification of the L4 intensity in the lymph glands of the indicated genotypes. The p-values were estimated with Student's t-test. In all figures, *p < 0.05; ***p < 0.001; ns, not significant.

mitotic and apoptotic hemocytes, the hemocytes were labeled for pH3 or Dcp-1, respectively. Detailed protocols are available in the Supplementary Methods.

Results

Sensitizing hemocytes enhances their response to Toll activation

To understand whether Gcm counteracts the Toll pro-inflammatory pathway, we combined a *Toll* mutation (16) and altered Gcm expression. $Toll^{10b}$ is a dominant mutation replacing the amino acid C781Y in the extracellular domain of the receptor, which induces constitutive activation of the Toll pathway (16). Compared to wild type, $Toll^{10b}$/+ animals display a higher number of hemocytes, precocious lymph gland histolysis, and spontaneous differentiation of lamellocytes that aggregate and form melanized black masses called melanotic tumors in 22% of the larvae (Figures 1B–E, F, J) (12, 17–20). In homeostatic conditions, the third larval instar lymph gland is composed of large primary lobes containing progenitors and differentiated hemocytes followed by small secondary lobes composed of undifferentiated hemocytes. In $Toll^{10b}$/+ animals, the primary lobes and some secondary lobes are histolyzed, and the remaining lobes are enlarged and display mature plasmatocytes and lamellocytes (Figures 1F, J; Supplementary Figures S1A, B) (12).

Knocking down Gcm expression in hemocytes using the *gcm-Gal4* driver (*gcm>gcm KD*) does not *per se* affect hemocyte number or nature (Figures 1D, E), but $Toll^{10b}$/*gcm>gcm KD* animals display a considerably enhanced inflammatory phenotype compared to $Toll^{10b}$/+ animals. The number of larvae carrying tumors (~40%) (Figure 1B) and the number of circulating hemocytes and lamellocytes per larva are significantly higher (Figures 1D, E). We did not observe significant differences of lamellocytes' differentiation in the remaining lobes of the double mutant $Toll^{10b}$/*gcm>gcm KD* compared to $Toll^{10b}$/+ lymph glands (Figures 1F–L). A similar strengthening of the melanotic tumor phenotype is observed by driving *gcm KD* with the driver *srp(hemo) Gal4* (*srp(hemo)>* (21) (Figure 1B), which is also specific for the first-wave hemocytes (22). Importantly, the phenotype of the double mutant animals is rescued by the overexpression of Gcm ($Toll^{10b}$/*gcm>gcm KD, gcm GOF*) (Figure 1B).

The response to Toll activation further increases in combination with the *gcm* null alleles (gcm^{26} (23) or the *Df(2L) 132* (24)) in heterozygous conditions. gcm^{26}/+;$Toll^{10b}$/+ and *Df(2L) 132*/+;$Toll^{10b}$/+ display higher penetrance of the melanotic tumor phenotype compared to $Toll^{10b}$/+ (Figure 1B). As in the case of *gcm KD*, the number of hemocytes in gcm^{26}/+ animals is not affected, while it does decrease in homozygous embryos (25, 26) (Figures 1D, E). gcm^{26}/+;$Toll^{10b}$/+ animals display a similar number of hemocytes but a higher proportion of lamellocytes in the hemolymph compared to $Toll^{10b}$/*gcm>gcm KD*, suggesting an even stronger pro-inflammatory phenotype than *gcm>gcm KD* (Figures 1B–E).

In sum, reducing *gcm* expression sensitizes the hemocytes and enhances the response to Toll pathway activation.

Transcriptome analysis of the sensitized hemocytes after Toll pathway activation

To assess the molecular mechanisms underlying the relative impact of Toll and Gcm on the observed phenotypes, we performed pairwise comparisons among the transcriptomes from gcm^{26}/+, from $Toll^{10b}$/+, and from gcm^{26}/+;$Toll^{10b}$/+ wandering third instar larvae (WL3) hemocytes (Supplementary Figures S2A, B).

The comparison of gcm^{26}/+;$Toll^{10b}$/+ with gcm^{26}/+ hemocytes highlights the impact of $Toll^{10b}$ on gene expression: 688 genes are significantly upregulated [mean expression >100, Log2 Fold change (Log2FC) >1, and $p < 0.01$] (Figure 2A, Supplementary Table S1). In line with the known function of the Toll pathway in response to fungi, bacteria, and wasp infestation (27–29), Gene Ontology (GO) analysis indicates the upregulation of genes involved in the innate immune response and more specifically in the Jak/Stat pathway in the defense response to Gram-positive and Gram-negative bacteria (Supplementary Figure S2C). The expression of most core components of the Toll pathway is induced, including that of the transcription factor *dorsal* (*dl*) (Figure 2A', Supplementary Figure S2F), in agreement with the autoregulatory loop shown for the Toll pathway (30). The induction of the core elements of the Jak/Stat pathway (Supplementary Figure S2D) is concordant with chromatin immunoprecipitation (ChIP) data targeting Dorsal (Dl), which indicates that Dl binds the promoters of all Jak/Stat core components (31). The response to Gram-negative bacteria is commonly associated with the activation of the Immune Deficiency (IMD) pathway and illustrates the crosstalk between the Toll and the IMD pathways (32–35). Most core components of the IMD pathways and the majority of antimicrobial peptides are upregulated in gcm^{26}/+;$Toll^{10b}$/+ compared to gcm^{26}/+ (Figures 2A'–A''', B), suggesting that the Toll pathway may activate the IMD pathway. Concordantly, ChIP data targeting Dl and Dorsal-related immunity factor (Dif) show that most genes of the IMD pathway are targeted by Dl/Dif in the larva (36), and a transcriptome analysis of $Toll^{10b}$ animals shows that Relish (Rel) is induced in $Toll^{10b}$ adults (33).

The impact of hemocyte sensitization is shown by comparing the transcriptomes from gcm^{26}/+;$Toll^{10b}$/+ and $Toll^{10b}$/+ larvae: 87 genes are downregulated and 161 genes are upregulated by gcm^{26} [mean expression >100, absolute value (Log2FC) >1, and $p < 0.01$] (Supplementary Table S1). Noteworthily, the number of genes affected by gcm^{26} is much lower than that affected by $Toll^{10b}$ (Figures 2A, C). This is likely due to the fact that $Toll^{10b}$ is a dominant gain-of-function (GOF) condition while gcm^{26} is a recessive mutation analyzed in heterozygous conditions, thus, a stronger impact on the transcriptome is expected for $Toll^{10b}$. With such a low number of genes, only a few GO terms were found significantly enriched when gcm^{26}/+;$Toll^{10b}$/+ and $Toll^{10b}$/+ larvae were compared. We did follow one of the GO terms with the lowest p-value, glutathione metabolic process (Supplementary Figure S2E), and found that most associated genes are downregulated in gcm^{26}/

10.3389/fimmu.2023.1293766

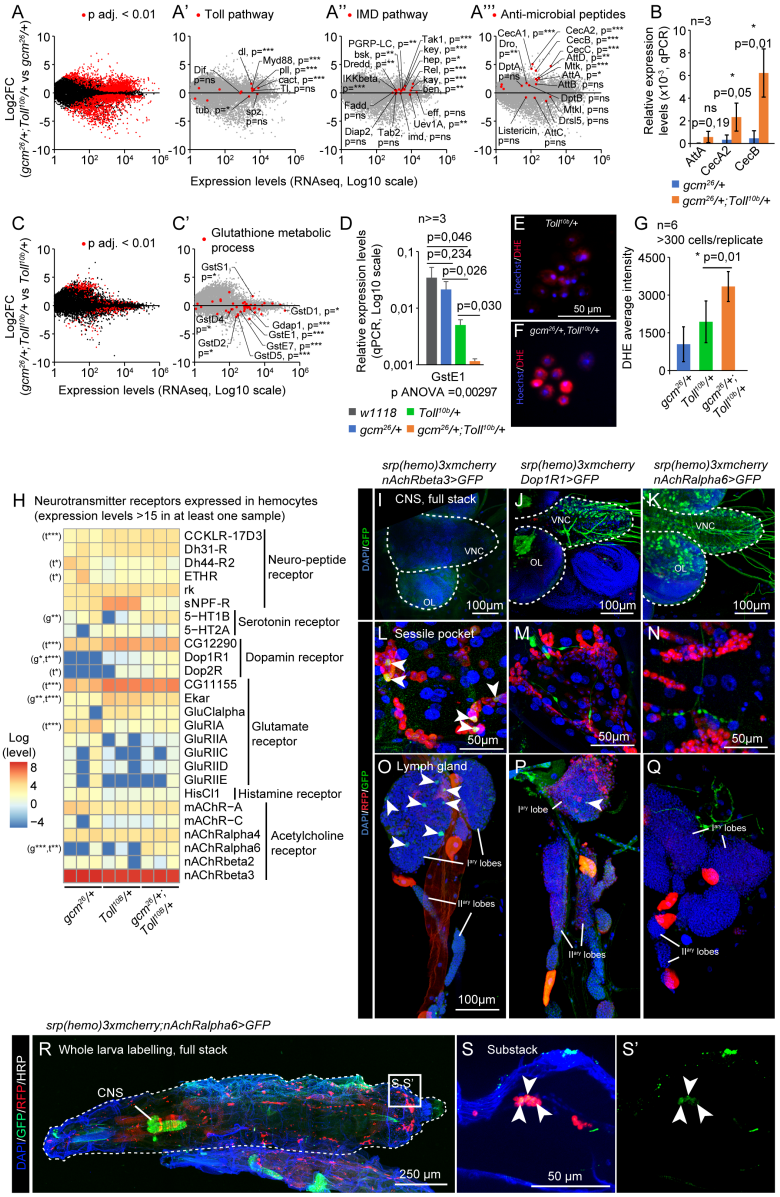

FIGURE 2

The pro-inflammatory condition *gcm*^{26}*/+;Toll*^{10b}*/+* induces the IMD pathway and modulates the ROS metabolism and the expression of neurotransmitter receptors. **(A–A''')** Transcriptome comparison of hemocytes from WL3 *gcm*^{26}*/+* and *gcm*^{26}*/+;Toll*^{10b}*/+*. The x-axis represents the average gene expression levels (n = 3) and the y-axis the Log2 fold change *gcm*^{26}*/+;Toll*^{10b}*/+/gcm*^{26}*/+*. The red dots highlight the genes presenting a significant fold change (adjusted p-values <0.01) in **(A)**, the genes of the Toll pathway in **(A')**, of the Immune Deficiency (IMD) pathway in **(A'')**, and the genes coding for antimicrobial peptides (AMP) in **(A''')**. **(B)** Expression levels of *AttA*, *CecA2*, and *CecB* in hemocytes *gcm*^{26} (in blue) and *gcm*^{26}*/+;Toll*^{10b}*/+* (in orange) estimated by quantitative PCR. N = 3 pools of 10 larvae, p-value estimated by bilateral Student's t-test. **(C, C')** Transcriptome comparison of hemocytes from WL3 *Toll*^{10b} and *gcm*^{26}*/+;Toll*^{10b}*/+*. The x-axis represents the average gene expression levels (n = 3) and the y-axis the Log2 fold change *gcm*^{26}*/+;Toll*^{10b}*/+/Toll*^{10b}. The red dots highlight the genes presenting a significant fold change (adjusted p-values <0.01) in **(C)** and the genes coding for glutathione S-transferase (Gst) in **(C')**. **(D)** Expression levels of *GstE1* in hemocytes *w1118* (wild-type control, in gray), *gcm*^{26}*/+* (in blue), *Toll*^{10b}*/+* (in green), and *gcm*^{26}*/+;Toll*^{10b}*/+* (in orange) estimated by quantitative PCR. N ≥ 3 pools of 10 larvae, p-value estimated by bilateral Student's t-test after ANOVA (p ANOVA = 0.00297). **(E–G)** Live hemocytes from *Toll*^{10b}*/+* **(E)** and *gcm*^{26}*/+;Toll*^{10b}*/+* **(F)** animals labeled for reactive oxygen species (ROS) using DHE (in red). The nuclei are labeled with Hoechst. The levels of oxidized DHE are quantified in **(G)**. N = 6, at least 300 hemocytes were monitored per replicate, the p-value was estimated by bilateral Student's t-test. **(H)** Heatmap representing the expression levels of neurotransmitter and neuropeptide receptors in hemocytes *gcm*^{26}*/+*, *Toll*^{10b}*/+*, and *gcm*^{26}*/+;Toll*^{10b}*/+*. The levels are in log scale. The significant p-values are mentioned on the left side of the heatmap. The comparison of *gcm*^{26}*/+* to *gcm*^{26}*/+;Toll*^{10b}*/+* is indicated by "t" and *Toll*^{10b}*/+* to *gcm*^{26}*/+;Toll*^{10b}*/+* by "g"; p-values: *: 0.05 < p < 0.01; **: 0.01 < p < 0.001; ***: 0.001 < p. **(I–Q)** Central nervous systems **(I–K)**, sessile pockets **(L–N)**, and lymph glands **(O–Q)** from larvae carrying the *T2A-Gal4* reporters of *nAchRbeta3*, *Dop1R1*, or *nAchRalpha6* (in green) and the hemocyte reporter *srp(hemo)3xmcherry* (in red). The nuclei are labeled with DAPI. The images were acquired with confocal microscopy and represent the whole stack projections. Scale bars are 100 µm in **(I–K)** and **(O–Q)** and 50 µm in **(L–N)**. **(R, S)** Whole-mount immunolabelings of L3 larvae *nAchRalpha6-T2A-Gal4/srp(hemo)3xmcherry;UAS-encGFP/+*. The larva is outlined by a white dashed line, the hemocytes are labeled with anti-RFP (in red), and the cells expressing *nAchRalpha6-T2A-Gal4* are labeled with anti-GFP (in green). The complete stack projections are shown in **(R)**, and a substack of the region indicated in panel R is shown in **(S, S')**.

10.3389/fimmu.2023.1293766

+;$Toll^{10b}$/+ compared to $Toll^{10b}$/+ hemocytes (Figures 2C', D) and belong to the Gst family. Since Gsts are involved in xenobiotic detoxification and in the defense mechanism against oxidative stress (37–39), we assessed the biological relevance of their reduction in hemocytes by estimating the ROS levels in gcm^{26}/+;$Toll^{10b}$/+ and $Toll^{10b}$/+ hemocytes using DHE. DHE is oxidized by intracellular ROS to produce red fluorescent ethidium (40). The quantification of the ethidium levels in hemocytes suggests higher levels of ROS in gcm^{26}/+;$Toll^{10b}$/+ than in $Toll^{10b}$/+ hemocytes, which can be due to the lower levels of Gst (Figures 2E–G). A recent study showed that the ROS produced after injury induces the Toll pathway in hemocytes (41). Thus, we speculate that the low levels of Gst in gcm^{26}/+;$Toll^{10b}$/+ hemocytes (Figure 2D) may increase their level of ROS, hence leading to a stronger response to Toll activation.

Unexpectedly, the GO term enrichment analyses carried out on each dataset highlighted GO terms related to synapse activity enriched in the two comparisons (Supplementary Figures S2C, E). These genes included several neurotransmitter receptors, suggesting an involvement of neurotransmitter-mediated signaling in Toll activation and gcm^{26} sensitization. A targeted analysis of neurotransmitter receptor expression in our dataset revealed the expression of 26 receptors in hemocytes and significant upregulations of the nicotinic acetylcholine receptor alpha 6 (nAchRalpha6), the serotonin receptor 5-hydroxytryptamine receptor 1B (5-HT1B), the dopamine receptor Dopamine 1-like receptor 1 (Dop1R1), and the short neuropeptide F receptor (sNPF-R) by $Toll^{10b}$ and/or by gcm^{26} (Figure 2H, Supplementary Table S1). The expression of nAchRalpha6, 5-HT1B, and Dop1R1 is significantly enhanced in the double mutant gcm^{26}/+;$Toll^{10b}$/+ compared to $Toll^{10b}$/+ and to gcm^{26}/+, with nAchRalpha6 showing the strongest increase. In contrast, sNPF-R is significantly reduced (Figure 2H, Supplementary Table S1). Other neurotransmitter receptors such as nAchRbeta3 are expressed constitutively at high levels in the hemocytes regardless of the genetic background (Figure 2H).

To verify the expression of neurotransmitter receptors in hemocytes, we took advantage of recently produced T2A reporter lines that express intact receptors along with Gal4 under the endogenous promoter of the gene (42, 43). We assessed the expression of *nAchRbeta3*, which presents the highest expression levels and is constitutively expressed in hemocytes (Figure 2H), as well as *Dop1R1* and *nAchRalpha6*, which show the most significant induction in the double mutant gcm^{26}/+;$Toll^{10b}$/+ compared to $Toll^{10b}$/+ and gcm^{26}/+. The *T2A-Gal4* lines were crossed with the double reporter *srp(hemo)-3xmcherry;UAS-GFP* to obtain flies that express Red Fluorescent Protein (RFP) in hemocytes (both lymph gland and first-wave hemocytes) (44) and Green Fluorescent Protein (GFP) in the receptor-T2A-Gal4 expressing cells. The *Dop1R1* and *nAchRalpha6* reporters but not *nAchRbeta3* are expressed in the larval central nervous system (CNS) (Figures 2I–K), consistent with the literature (42, 45).

The *nAchRbeta3* reporter shows GFP signals in hemocytes from the lymph gland and in sessile pockets (Figures 2L, O), and the *Dop1R1* reporter is detected in a few cells of the lymph gland but not in the hemocytes of the sessile pockets (Figures 2M, P) nor in other circulating or resident hemocytes. The *nAchRalpha6-T2A-Gal4* reporter is not detected in the sessile pockets nor in the lymph gland (Figures 2N, Q); however, whole-larva immunolabeling and larval filet preparations show the expression of the receptor in resident hemocytes located in the dorsal stripes (Figure 1A; Figures 2R, S; Supplementary Figures S3A–C). The larva contains on average 1.05% ± 0.49% of nAchRalpha6-positive hemocytes (n = 3, estimated by cytometry on 10 larvae per replicate). Because of the highest effect observed in the double mutant larvae, we focused on *nAchRalpha6* and confirmed its expression profile with a transgenic line expressing a nAchRalpha6-YFP fusion protein (46) (Supplementary Figures S3D–S3F'''). The nAchRalpha6-positive hemocytes express strongly the plasmatocyte markers Nimrod C1 (NimC1 or P1) and Hemese (He) (Supplementary Figures S3C–S3F'''). At last, we profiled nAchRalpha6 in gcm^{26}/+;$Toll^{10b}$/+, $Toll^{10b}$/+, and gcm^{26}/+ larvae by crossing in *nAchRalpha6-T2A-Gal4;UAS-nRFP*. The larval filets show that the double mutants gcm^{26}/+;$Toll^{10b}$/+ have more *nAchRalpha6* hemocytes than control, $Toll^{10b}$/+, and gcm^{26}/+ larvae, confirming the transcriptomic data (Supplementary Figures S3G–K).

Overall, these data suggest that Toll activation regulates the IMD and the Jak/Stat pathways, that sensitized hemocytes display higher ROS levels in response to Toll activation possibly due to suboptimal levels of Gst, and that the hemocytes express neurotransmitter receptors whose expression is modulated by inflammatory conditions.

nAchRalpha6 modulates the proliferation of hemocytes

We next evaluated the impact of the receptors on hemocytes. We focused on *nAchRalpha6* and observed how manipulating its expression levels affects hemocytes. The null mutation $nAchRalpha6^{DAS1}$ alters the splice donor site of the first intron, which produces an inactive truncated protein, and the null mutation $nAchRalpha6^{DAS2}$ converts the codon for the tryptophan 458 to a terminal codon. In both mutations, the number of hemocytes in WL3 is significantly reduced (Figure 3A). Given the impact of *nAchRalpha6* in the nervous system (49), we next determined if the phenotype is cell autonomous by downregulating the expression of *nAchRalpha6* specifically in hemocytes. The expression of a *UAS-RNAi* transgene targeting the receptor was driven by a combination of the two larval hemocyte-specific drivers *HmldeltaGal4* and *PxnGal4* that cover the whole larval hemocyte population (50–52). The *nAchRalpha6* knockdown (*nAchRalpha6-KD*) animals are completely viable and display fewer hemocytes than the control animals (Figure 3B). The hemocyte number is also reduced in *nAchRalpha6-KD* with the driver *PxnGal4* alone (Figure 3C), but not with *HmldeltaGal4* alone (Figure 3D). The two drivers are specific to hemocytes, and while the majority of hemocytes express both drivers, small subsets of hemocytes express exclusively *PxnGal4* (37% in WL3) or *HmldeltaGal4* (10% in WL3) (50). The different hemocyte number observed upon *nAchRalpha6 KD* driven by one or the other driver may depend either on the different hemocyte populations affected or on the different levels of knockdown. To discern between the two possibilities, we stabilized and hence enhanced *HmldeltaGal4*-driven expression levels using the G-trace approach (47). *HmldeltaGal4,Dbgtrace>nAchRalpha6-KD* animals do display

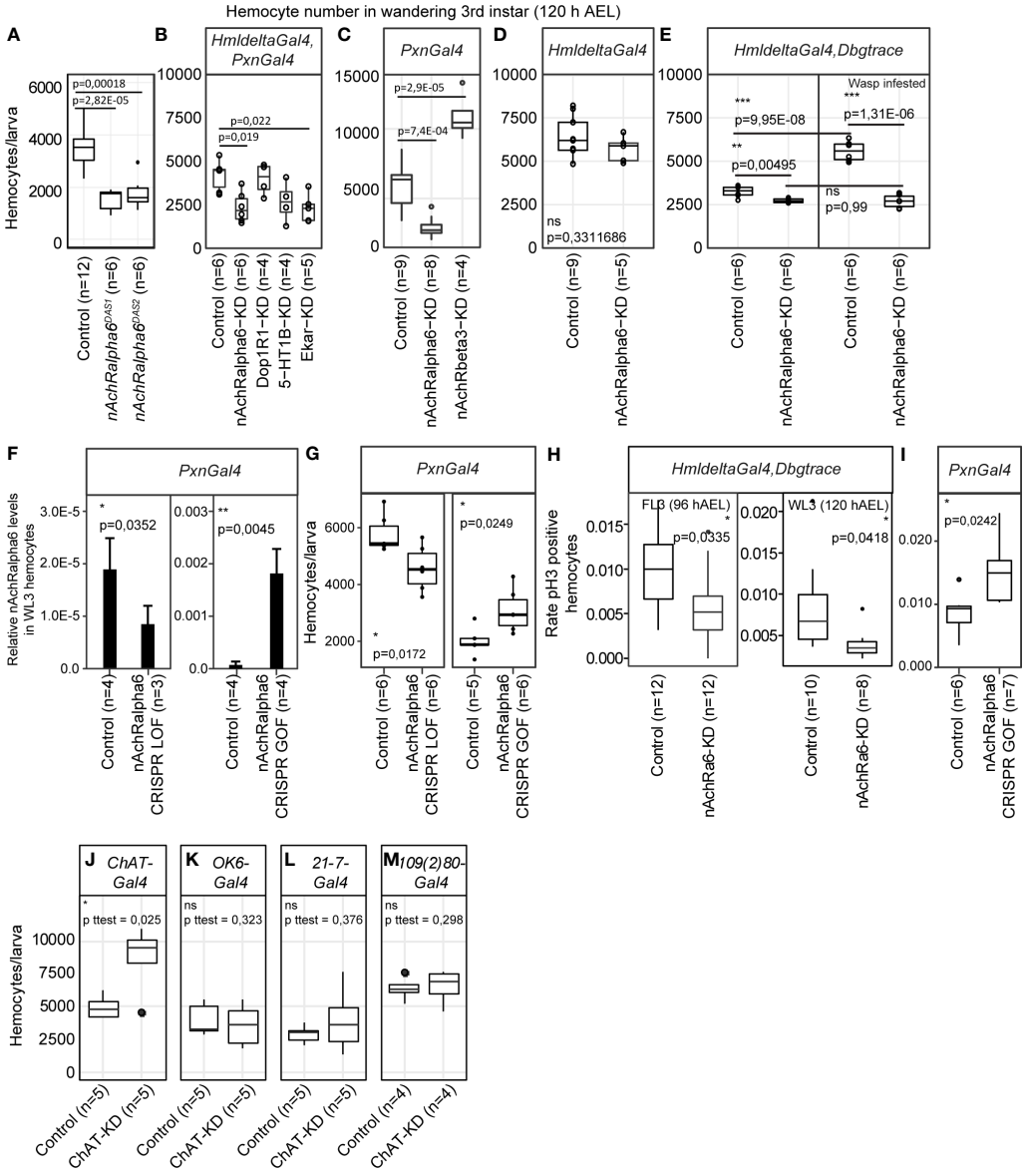

FIGURE 3
nAchRalpha6 modulates hemocyte proliferation, cell autonomously. **(A–E)** Number of hemocytes per WL3 in the indicated genotypes. N ≥ 4, each replicate being a pool of 10 females. Note that in *HmldeltaGal4,Dbgtrace* **(E)**, Gal4 expression was enhanced using lineage tracing *Gal4* transgenes (*Dbgtrace*). *Dbgtrace* includes a flipase cassette under the control of the UAS promoter (*UAS-FLP*) and the *Gal4* gene separated from the *Act5C* constitutive promoter by a stop cassette surrounded by two flipase recognition sites (*Act5C-FRT-STOP-FRT-Gal4*) (47). The expression of the flipase in the hemocytes excises the STOP cassette and leads to constitutive expression of *Gal4* in those cells, strongly enhancing the expression levels of *Gal4*. The p-values were estimated by one-factor ANOVA followed by *post-hoc* Tukey HSD for **(A–C)** (p ANOVA **(A)** = 7.17E-06; **(B)** = 0.0051787; **C** = 5.32E-08) and by Student's t-test after variance analysis for **(D, E)**. **(F)** Expression levels of *nAchRalpha6* in WL3 hemocytes from *Pxn>nAchRalpha6 CRISPR LOF* and *GOF* animals (complete genotypes are indicated in the *Methods* section) measured by quantitative PCR; n = 4 each replicate being a pool of 10 females. Note that the controls are specific to each genetic setup. The full genotypes of the controls are indicated in the *Methods* section *Fly Strains and Genetics*. In *CRISPR LOF* animals, the Cas9 nuclease was expressed specifically in hemocytes using the driver *PxnGal4* and targeted to the coding sequence of *nAchRalpha6* by the constitutive expression of two *nAchRalpha6* specific guide RNA (*nAchRalpha6 CRISPR LOF*) (48). In *CRISPR GOF* animals, a dead Cas9 fused to the activator domain VPR (Zirin et al., 2020) was expressed with the driver *PxnGal4* and guided to the promoter of *nAchRalpha6* with specific guide RNA (*nAchRalpha6 CRISPR GOF*). Note that the two controls are different: *Pxn>nAchRalpha6 CRISPR LOF* Control is *UAS-Cas9/+;PxnGal4/+* and *Pxn>nAchRalpha6 CRISPR GOF* Control is *UAS- dCas9-VPR/+;PxnGal4/+* (see Supplementary Methods). **(G)** Number of hemocytes per WL3 in *Pxn>nAchRalpha6 CRISPR LOF* and *GOF*. N ≥ 5, each replicate being a pool of 10 females. **(H)** Quantification of the proliferative hemocytes in feeding L3 (96 hAEL) and WL3 (120 hAEL) *HmldeltaGal4,Dbgtrace* or *HmldeltaGal4,Dbgtrace, nAchRalpha6-KD*; n ≥ 8, with more than 300 hemocytes scored for each replicate, p-values were estimated by one-factor ANOVA. **(I)** Quantification of the proliferative hemocytes in WL3 (120 hAEL) *Pxn>nAchRalpha6 CRISPR GOF* and control; n ≥ 6, with more than 1,000 hemocytes scored for each replicate, p-value was estimated by one-factor ANOVA. **(J–M)** Number of hemocytes per WL3 (120 hAEL) in the indicated genotypes. ChAT expression was inhibited specifically in cholinergic neurons with ChATGal4 **(J)**, in type I motoneurons with OK6Gal4 **(K)** and in multidendritic neurons with 21-7Gal4 or 109(2)80Gal4 **(L, M)**. N ≥ 4, each replicate being a pool of 10 females.

10.3389/fimmu.2023.1293766

fewer hemocytes compared to the control WL3 (Figure 3E), indicating that the difference observed upon *PxnGal4* and *HmldeltaGal4*-driven knockdown is due to different levels of Gal4 induction.

To further prove the role of *nAchRalpha6* in hemocytes, we used tissue-specific Clustered Regularly Interspaced Short Palindromic Repeats / CRISPR-associated protein 9 (CRISPR/Cas9)-mediated loss-of-function (LOF) and GOF animals (Figures 3F, G). In *nAchRalpha6 CRISPR LOF* larvae, the expression levels of nAchRalpha6 decrease and so does the number of hemocytes (Figures 3F, G). In *nAchRalpha6 CRISPR GOF*, the expression levels of nAchRalpha6 increase by more than 10-fold and the number of hemocytes increases compared to those of the control (Figures 3F, G). Altogether, these data demonstrate that nAchRalpha6 regulates the number of hemocytes in the larva.

To assess the cause(s) of the different hemocyte numbers in *nAchRalpha6 KD* and *GOF*, we quantified hemocyte proliferation and apoptosis using antibodies against phosphorylated Ser10 of histone 3 (pH3) (53) and cleaved caspase Dcp-1 (54), respectively. No difference was found in the rate of apoptosis (Supplementary Figures S4B–D). A significant reduction of the proliferation rate was observed in *nAchRalpha6-KD* hemocytes in feeding as well as in wandering third instar larvae (FL3, WL3, respectively) and a significant increase in proliferation in *nAchRalpha6 CRISPR GOF* hemocytes compared to control hemocytes (Figures 3H, I; Supplementary Figure S4A). To assess if the impact of nAchRalpha6 on proliferation is cell autonomous, we quantified the number of proliferative hemocytes that express nAchRalpha6 in *nAchRalpha6-T2A-Gal4/+;UAS-GFP/srp(hemo)3xmcherry* larvae. On average, 26.6% ± 2.6% of nAchRalpha6 hemocytes are mitotic according to pH3 labeling compared to 0.6% in the whole population (n = 3, estimated on 10 larvae per replicate, p paired Student's t-test = 0.0038). The nAchRalpha6 hemocytes represent 46% ± 6.5% of the proliferative larval hemocytes, suggesting that the receptor is involved in the cell autonomous regulation of hemocyte proliferation. These results are in agreement with the increase in hemocyte number observed in the gcm^{26}/+;$Toll^{10b}$/+ larvae that also display increased expression of *nAchRalpha6*. We hence assessed the direct impact of nAchRalpha6 on hemocyte number in inflammatory conditions. Given the complexity of the genetic setup to reduce *nAchRalpha6* expression in $Toll^{10b}$ animals, we induced an immune challenge upon infesting larvae with the parasitoid wasp *Leptopilina boulardi*, which is known to trigger the Toll pathway. The rate of lamellocyte differentiation is not affected in *HmldeltaGal4, Dbgtrace>nAchRalpha6-KD* animals, with a percentage of lamellocytes/total hemocytes number of 18.6% (n = 6, stdev. = 2.9%) compared to 18.4% in control animals (n = 6, stdev = 12.3%; p t-test unequal variance = 0.97). However, a striking difference is observed in the number of hemocytes. Control animals display significantly more hemocytes after wasp infestation, while the hemocyte number in *nAchRalpha6-KD* animals remains stable (Figure 3E). Thus, the increase of hemocyte triggered by wasp infestation depends at least in part on *nAchRalpha6* expression in hemocytes.

Overall, these data show that *nAchRalpha6* modulates the proliferation of hemocytes in homeostasis and during the inflammatory response.

Cholinergic signaling regulates hemocyte homeostasis

We evaluated the impact of other neurotransmitter receptors and downregulated 5-HT1B, Dop1R1, nAchRbeta3 or the glutamate receptor Eye-enriched kainate receptor (Ekar) (Figure 3B). In all cases, the KD animals are completely viable (data not shown). In terms of hemocyte number, *5-HT1B-KD* and *Dop1R1-KD* show no difference compared to control WL3. *Ekar-KD* displays less hemocytes (Figure 3B), suggesting that glutamate signaling may also be involved in the regulation of hemocyte homeostasis. *nAchRbeta3-KD* shows a strong increase in the number of hemocytes (Figure 3C), which further highlights the importance of cholinergic signaling in hemocyte homeostasis.

At last, to assess the impact of cholinergic transmission on hemocytes, we monitored the number of larval hemocytes after inhibiting the expression of the choline-acetyltransferase ChAT in neurons. To inhibit ChAT, we used a *UAS-ChAT-RNAi* (55) and a *ChAT-Gal4* to drive *ChAT-RNAi* in the cholinergic neurons (56), which led to a strong increase in the number of hemocytes (Figure 3J), indicating that cholinergic neurons modulate hemocyte homeostasis through the secretion of acetylcholine. As controls, we used *OK6-Gal4* for type 1 motoneurons (57), which mostly secrete glutamate (58, 59), *21-7-Gal4* and *109(2)80-Gal4* drivers for multidendritic neurons, which are cholinergic (56) and regulate hemocyte localization and proliferation at the dorsal stripes through activin signaling (60). Since the multidendritic neurons make synapses at the CNS (61–64), we do not expect an effect using these drivers either (Figures 3K–M). These data indicate that motoneurons or multidendritic neurons are not the source of acetylcholine that affects the hemocyte number.

Taken together, our data show that several neurotransmitter receptors are involved in hemocyte homeostasis, that nAchRalpha6 regulates the proliferation of the hemocyte cell autonomously, and that acetylcholine signaling to the hemocytes likely originates from cholinergic neurons from the CNS.

Discussion

In this study, we show that downregulating Gcm enhances the immune response to Toll activation, calling for a general anti-inflammatory role of this evolutionarily conserved transcriptional cascade. The comparison of the transcriptomes in control and mutant backgrounds reveals that the activation of the Toll pathway induces the expression of core components of the IMD pathway and that sensitizing the hemocytes by Gcm downregulation alters the levels of Gst and ROS metabolism in $Toll^{10b}$ background. Finally, we demonstrate that hemocyte expression of acetylcholine receptor nAchRalpha6 is modulated upon hemocyte sensitizing and Toll activation and that nAchRalpha6 regulates hemocyte proliferation cell autonomously. The finding that cholinergic signaling controls hemocyte proliferation underlines the interaction between the immune and nervous systems.

Sensitized hemocytes display an enhanced response to Toll and Jak/Stat signaling

Gcm acts as a general anti-inflammatory factor, as its downregulation enhances the inflammatory response to challenges of different natures. This phenotype is observed in sensitized hemocytes upon the constitutive activation of the Toll pathway (this study) or of the Jak/Stat pathway (13), two examples of chronic challenges. A similar phenotype is also observed upon wasp infestation, an acute challenge that activates both pathways (13, 29). The inflammatory responses induced by Toll and Jak/Stat are highly similar: increasing hemocyte number and lamellocyte differentiation at comparable levels (13). In both conditions, sensitizing the hemocytes doubles the penetrance of the melanotic tumor phenotype in the larva (13). These strong similarities can be explained by the high interconnection between the two pathways. For example, the Toll pathway acts upstream of Jak/Stat for the regulation of the thiolester-containing protein Tep1 (65). In addition, the Tep protein family regulates the Toll pathway (66) and Jak/Stat modulates the expression of the Toll's ligand Spatzle (67), providing means by which the Jak/Stat pathway can modulate the Toll pathway. At last, recent data show that in hemocytes, Toll activation induces the expression of the pro-inflammatory cytokine Upd3, which activates the Jak/Stat pathway (68). Therefore, the activation of one pathway will likely activate the second one in a feed-forward loop. This hypothesis is supported by the *Toll*^{10b} transcriptome that shows increased levels of several targets regulated by the Jak/Stat pathway, including Ptp61F and Socs36E (69) (Supplementary Figure S2D) as well as Tep1, Tep2, and Tep4 (65, 67) (Supplementary Table S1). Our previous data showed that Gcm inhibits the Jak/Stat pathway (13). Gcm could hence inhibit the Toll pathway at least in part through the inhibition of the Jak/Stat pathway.

A second hypothesis that can explain the impact of Gcm on the inflammatory response is the modulation of the Gst. Our transcriptome analysis on the sensitized animals reveals a significant decrease in the anti-oxidant enzymes Gst, which correlates with higher levels of ROS. The production of ROS is tightly linked to the Toll pathway. On the one hand, ROS are known to activate the Toll and the Jak/Stat pathways (41, 70); on the other hand, Toll activates the production of ROS (71). We speculate that in our sensitized model, the deficit in Gst increases ROS levels, which might enhance the inflammatory response induced by Toll activation.

These data highlight Gcm as a potent anti-inflammatory transcription factor acting at multiple levels, directly on the Jak/Stat pathway, indirectly on Toll and IMD pathway or on ROS levels through the modulation of the Gst. Importantly, the impact of Gcm on the inflammatory response of immune cells is conserved in mammals. In mice, knockout for Gcm2 in microglia, the macrophage of the nervous system leads to the production of microglia in a pro-inflammatory state (14).

Expression of neurotransmitter receptors in hemocytes

The modulation of the immune cells by neurotransmitters is well described in mammals. Numerous neurotransmitter receptors are expressed in immune cells, and cholinergic, dopaminergic, and serotoninergic signaling mediates the function, the inflammatory status, and the proliferation of macrophages [reviewed by (72)]. In *Drosophila*, few studies report neurotransmitter signaling in immune cells. Neuronal gamma aminobutyric acid (GABA) is secreted in the hemolymph after olfactory stimuli induced by parasitoid wasp scent and promotes the differentiation of lamellocytes in the lymph gland (73). Qi et al. (74) showed the impact of serotonin signaling on the phagocytic capacity of the plasmatocytes in the butterfly *Pieris rapae* and in *Drosophila*. Immune challenge in the adult induces the secretion of serotonin by the plasmatocytes, which enhances their phagocytic capacity. This autocrine process is mediated by the receptors 5-HT1B and 5-HT2B (74). At last, dopamine signaling is used by the progenitors in the lymph gland to regulate the cell cycle (75).

Our transcriptome analysis reveals the expression of a dozen neurotransmitter receptors in the hemocytes, some of whose appear to be modulated by the inflammatory state of the larva. We report here the expression of receptors to acetylcholine, glutamate, serotonin, dopamine, and several neuropeptides in the hemocytes patrolling the larva. Our data indicate that the levels of nAchRalpha6 increase in sensitized hemocytes in *Toll*^{10b} background and that nAchRalpha6 is enriched in proliferative hemocytes. Additionally, we have shown that modulating acetylcholine production in the nervous system or the expression of specific subunits of the acetylcholine receptors in the hemocytes has a significant impact on these cells. Repressing cholinergic signaling from the neurons increases the number of hemocytes, similar to the effect of inhibiting *nAchRbeta3* or overexpressing *nAchRalpha6* in hemocytes and opposite to the effect of inhibiting *nAchRalpha6* in hemocytes (Figure 3C). Taken together, these data indicate that cholinergic signaling regulates the proliferation of hemocytes through the activation of nicotinic acetylcholine receptors. The nicotinic acetylcholine receptor is composed of five subunits homomeric or heterodimeric (76), and the subunit composition defines its biochemical properties (77). Our experimental setup modulates the expression of specific subunits, which may modify the composition of the receptors in the hemocytes and lead to two distinct effects (i.e., promotion or inhibition of hemocyte proliferation with nAchRalpha6 or nAchRbeta3, respectively). Thus, modulating the expression of neurotransmitter receptor subunits may represent a novel mechanism by which the hemocyte homeostasis is regulated in response to pro-inflammatory cues.

Altogether, these observations suggest that hemocytes are sensitive to a large panel of neurotransmitters. Our data do not allow to distinguish if the signal is transmitted through direct neuron–hemocyte connection or through systemic acetylcholine secretion. Several neurotransmitters are secreted systemically in the hemolymph (73) and can be produced by the hemocytes themselves (74, 75), but this was never shown for acetylcholine in the hemolymph, and our transcriptomic data indicate that ChAT is not expressed in hemocytes. A recent study in adult *Drosophila* shows that tissues other than neurons produce acetylcholine and that both neuronal and glia-derived acetylcholine regulates the Toll-mediated immune response of hemocytes through nAch receptors (78). Thus, cholinergic signaling appears as a fundamental mechanism of the immune response, providing a direct

communication channel between the nervous system and the immune system. Establishing the prevalence, the localization, and the nature of the receptors expressed in the hemocytes and the source of the neurotransmitters will be key steps to decipher this signaling axis.

Concluding notes

Our study ascertains the anti-inflammatory role of Gcm on several inflammatory pathways, reveals a role for nAchRalpha6 in the regulation of hemocyte proliferation in homeostasis as well as in response to inflammation, and shows the contribution of the neuronal cholinergic signaling to the immune system homeostasis. These data parallel the function of neurotransmitter receptors in mammals, whose activation in macrophages modulates cell proliferation and the activity of inflammatory pathways. Our model paves the way to characterize the role of neurotransmitter signaling in the immune response and to explore the evolutionary conserved mechanisms involved.

Data availability statement

The datasets presented in this study can be found in online repositories. The names of the repository/repositories and accession number(s) can be found below: https://www.ebi.ac.uk/arrayexpress/, E-MTAB-11970.

Ethics statement

Ethical review and approval was not required for the study on animals in accordance with the local legislation and institutional requirements.

Author contributions

WB: Conceptualization, Data curation, Formal Analysis, Investigation, Methodology, Writing – original draft. SM: Data curation, Investigation, Writing – review & editing. CD: Investigation, Methodology, Writing – review & editing. CR: Methodology, Validation, Writing – review & editing. AG: Conceptualization, Formal Analysis, Funding acquisition, Project administration, Resources, Supervision, Validation, Writing – review & editing. PC: Conceptualization, Data curation, Formal Analysis, Funding acquisition, Investigation, Methodology, Project administration, Supervision, Validation, Writing – original draft, Writing – review & editing.

Funding

The author(s) declare financial support was received for the research, authorship, and/or publication of this article. This work was supported by INSERM, CNRS, UDS, Ligue Régionale contre le Cancer, Hôpital de Strasbourg, ARC, CEFIPRA, USIAS, FRM and ANR grants. PC was funded by the ANR and by the ARSEP, WB by the USIAS and by the FRM (FDT20160435111). SM was funded from CEFIPRA and ANR fellowships. This work of the Interdisciplinary Thematic Institute IMCBio, as part of the ITI 2021-2028 program of the University of Strasbourg, CNRS and Inserm, was supported by IdEx Unistra (ANR-10-IDEX-0002), and by SFRI-STRAT'US project (ANR 20-SFRI-0012) and EUR IMCBio (ANR-17-EURE-0023) under the framework of the French Investments for the Future Program.

Acknowledgments

We thank K. Bruckner, D. Siekhaus, D. Hultmark, H. Tanimoto, S. Kondo, S. Russell, V. Honti, I. Ando and P. Soba for providing fly stocks and antibodies. In addition, stocks obtained from the Bloomington *Drosophila* Stock Center (NIH P40OD018537) and antibodies obtained from the Developmental Studies Hybridoma Bank created by the NICHD of the NIH and maintained at The University of Iowa (Department of Biology, Iowa City, IA 52242) were used in this study. We thank F. Stenger, M. Heinis, M. Moog, A. Kucan, A. Bhan, E. Naegelen, G. Zhang for technical assistance. We thank the Imaging Center of the IGBMC for technical assistance. We thank A. Maglott-Roth from the IGBMC screening facility for the hemocyte analysis. The sequencing was performed by the GenomEast platform, a member of the "France Génomique" consortium (ANR-10-INBS-0009).

Conflict of interest

The authors declare that the research was conducted in the absence of any commercial or financial relationships that could be construed as a potential conflict of interest.

Publisher's note

Supplementary material

The Supplementary Material for this article can be found online at: https://www.frontiersin.org/articles/10.3389/fimmu.2023.1293766/full#supplementary-material.

References

1. Nathan C, Ding A. Nonresolving inflammation. *Cell* (2010) 140(6):871–82. doi: 10.1016/j.cell.2010.02.029

2. Greten FR, Grivennikov SI. Inflammation and cancer: triggers, mechanisms, and consequences. *Immunity* (2019) 51(1):27–41. doi: 10.1016/j.immuni.2019.06.025

3. Fakhoury M. Immune-mediated processes in neurodegeneration: where do we stand? *J Neurol* (2016) 263(9):1683–701. doi: 10.1007/s00415-016-8052-0

4. Imler JL. Overview of Drosophila immunity: a historical perspective. *Dev Comp Immunol* (2014) 42(1):3–15. doi: 10.1016/j.dci.2013.08.018

5. Imler JL, Hoffmann JA. Signaling mechanisms in the antimicrobial host defense of Drosophila. *Curr Opin Microbiol* (2000) 3(1):16–22. doi: 10.1016/S1369-5274(99)00045-4

6. Lemaitre B, Hoffmann J. The host defense of Drosophila melanogaster. *Annu Rev Immunol* (2007) 25:697–743. doi: 10.1146/annurev.immunol.25.022106.141615

7. Arbouzova NI, Zeidler MP. JAK/STAT signalling in Drosophila: insights into conserved regulatory and cellular functions. *Development* (2006) 133(14):2605–16. doi: 10.1242/dev.02411

8. Lang T, Mansell A. The negative regulation of Toll-like receptor and associated pathways. *Immunol Cell Biol* (2007) 85(6):425–34. doi: 10.1038/sj.icb.7100094

9. Gold KS, Bruckner K. Macrophages and cellular immunity in Drosophila melanogaster. *Semin Immunol* (2015) 27(6):357–68. doi: 10.1016/j.smim.2016.03.010

10. Banerjee U, Girard JR, Goins LM, Spratford CM. Drosophila as a genetic model for hematopoiesis. *Genetics* (2019) 211(2):367–417. doi: 10.1534/genetics.118.300223

11. Mase A, Augsburger J, Bruckner K. Macrophages and their organ locations shape each other in development and homeostasis - A drosophila perspective. *Front Cell Dev Biol* (2021) 9:630272. doi: 10.3389/fcell.2021.630272

12. Davidson CJ, Tirouvanziam R, Herzenberg LA, Lipsick JS. Functional evolution of the vertebrate Myb gene family: B-Myb, but neither A-Myb nor c-Myb, complements Drosophila Myb in hemocytes. *Genetics* (2005) 169(1):215–29. doi: 10.1534/genetics.104.034132

13. Bazzi W, Cattenoz PB, Delaporte C, Dasari V, Sakr R, Yuasa Y, et al. Embryonic hematopoiesis modulates the inflammatory response and larval hematopoiesis in Drosophila. *Elife* (2018) 7. doi: 10.7554/eLife.34890

14. Pavlidaki A, Panic R, Monticelli S, Riet C, Yuasa Y, Cattenoz PB, et al. An anti-inflammatory transcriptional cascade conserved from flies to humans. *Cell Rep* (2022) 41(3):111506. doi: 10.1016/j.celrep.2022.111506

15. Zhao H, Joseph J, Fales HM, Sokoloski EA, Levine RL, Vasquez-Vivar J, et al. Detection and characterization of the product of hydroethidine and intracellular superoxide by HPLC and limitations of fluorescence. *Proc Natl Acad Sci U S A* (2005) 102(16):5727–32. doi: 10.1073/pnas.0501719102

16. Schneider DS, Hudson KL, Lin TY, Anderson KV. Dominant and recessive mutations define functional domains of Toll, a transmembrane protein required for dorsal-ventral polarity in the Drosophila embryo. *Genes Dev* (1991) 5(5):797–807. doi: 10.1101/gad.5.5.797

17. Minakhina S, Steward R. Melanotic mutants in Drosophila: pathways and phenotypes. *Genetics* (2006) 174(1):253–63. doi: 10.1534/genetics.106.061978

18. Huang L, Ohsako S, Tanda S. The lesswright mutation activates Rel-related proteins, leading to overproduction of larval hemocytes in Drosophila melanogaster. *Dev Biol* (2005) 280(2):407–20. doi: 10.1016/j.ydbio.2005.02.006

19. Remillieux-Leschelle N, Santamaria P, Randsholt NB. Regulation of larval hematopoiesis in Drosophila melanogaster: a role for the multi sex combs gene. *Genetics* (2002) 162(3):1259–74. doi: 10.1093/genetics/162.3.1259

20. Zettervall CJ, Anderl I, Williams MJ, Palmer R, Kurucz E, Ando I, et al. A directed screen for genes involved in Drosophila blood cell activation. *Proc Natl Acad Sci U S A* (2004) 101(39):14192–7. doi: 10.1073/pnas.0403789101

21. Bruckner K, Kockel L, Duchek P, Luque CM, Rorth P, Perrimon N. The PDGF/VEGF receptor controls blood cell survival in Drosophila. *Dev Cell* (2004) 7(1):73–84. doi: 10.1016/j.devcel.2004.06.007

22. Cattenoz PB, Sakr R, Pavlidaki A, Delaporte C, Riba A, Molina N, et al. Temporal specificity and heterogeneity of Drosophila immune cells. *EMBO J* (2020) 39(12):e104486. doi: 10.15252/embj.2020104486

23. Vincent S, Vonesch JL, Giangrande A. Glide directs glial fate commitment and cell fate switch between neurones and glia. *Development* (1996) 122(1):131–9. doi: 10.1242/dev.122.1.131

24. Kammerer M, Giangrande A. Glide2, a second glial promoting factor in Drosophila melanogaster. *EMBO J* (2001) 20(17):4664–73. doi: 10.1093/emboj/20.17.4664

25. Bernardoni R, Vivancos V, Giangrande A. glide/gcm is expressed and required in the scavenger cell lineage. *Dev Biol* (1997) 191(1):118–30. doi: 10.1006/dbio.1997.8702

26. Alfonso TB, Jones BW. gcm2 promotes glial cell differentiation and is required with glial cells missing for macrophage development in Drosophila. *Dev Biol* (2002) 248(2):369–83. doi: 10.1006/dbio.2002.0740

27. Rutschmann S, Kilinc A, Ferrandon D. Cutting edge: the toll pathway is required for resistance to gram-positive bacterial infections in Drosophila. *J Immunol* (2002) 168(4):1542–6. doi: 10.4049/jimmunol.168.4.1542

28. Louradour I, Sharma A, Morin-Poulard I, Letourneau M, Vincent A, Crozatier M, et al. Reactive oxygen species-dependent Toll/NF-kappaB activation in the Drosophila hematopoietic niche confers resistance to wasp parasitism. *Elife* (2017) 6. doi: 10.7554/eLife.25496

29. Kim-Jo C, Gatti JL, Poirie M. Drosophila cellular immunity against parasitoid wasps: A complex and time-dependent process. *Front Physiol* (2019) 10:603. doi: 10.3389/fphys.2019.00603

30. Mrinal N, Nagaraju J. Dynamic repositioning of dorsal to two different kappaB motifs controls its autoregulation during immune response in Drosophila. *J Biol Chem* (2010) 285(31):24206–16. doi: 10.1074/jbc.M109.097196

31. MacArthur S, Li XY, Li J, Brown JB, Chu HC, Zeng L, et al. Developmental roles of 21 Drosophila transcription factors are determined by quantitative differences in binding to an overlapping set of thousands of genomic regions. *Genome Biol* (2009) 10(7):R80. doi: 10.1186/gb-2009-10-7-r80

32. Valanne S, Wang JH, Ramet M. The Drosophila Toll signaling pathway. *J Immunol* (2011) 186(2):649–56. doi: 10.4049/jimmunol.1002302

33. De Gregorio E, Spellman PT, Tzou P, Rubin GM, Lemaitre B. The Toll and Imd pathways are the major regulators of the immune response in Drosophila. *EMBO J* (2002) 21(11):2568–79. doi: 10.1093/emboj/21.11.2568

34. Nishide Y, Kageyama D, Yokoi K, Jouraku A, Tanaka H, Futahashi R, et al. Functional crosstalk across IMD and Toll pathways: insight into the evolution of incomplete immune cascades. *Proc Biol Sci* (2019) 286(1897):20182207. doi: 10.1098/rspb.2018.2207

35. Alejandro AD, Lilia JP, Jesus MB, Henry RM. The IMD and Toll canonical immune pathways of Triatoma pallidipennis are preferentially activated by Gram-negative and Gram-positive bacteria, respectively, but cross-activation also occurs. *Parasit Vectors* (2022) 15(1):256. doi: 10.1186/s13071-022-05363-y

36. Kudron MM, Victorsen A, Gevirtzman L, Hillier LW, Fisher WW, Vafeados D, et al. The modERN resource: genome-wide binding profiles for hundreds of drosophila and caenorhabditis elegans transcription factors. *Genetics* (2018) 208(3):937–49. doi: 10.1534/genetics.117.300657

37. Hurst R, Bao Y, Jemth P, Mannervik B, Williamson G. Phospholipid hydroperoxide glutathione peroxidase activity of human glutathione transferases. *Biochem J* (1998) 332(Pt 1):97–100. doi: 10.1042/bj3320097

38. Armstrong RN. Glutathione S-transferases: reaction mechanism, structure, and function. *Chem Res Toxicol* (1991) 4(2):131–40. doi: 10.1021/tx00020a001

39. Sawicki R, Singh SP, Mondal AK, Benes H, Zimniak P. Cloning, expression and biochemical characterization of one Epsilon-class (GST-3) and ten Delta-class (GST-1) glutathione S-transferases from Drosophila melanogaster, and identification of additional nine members of the Epsilon class. *Biochem J* (2003) 370(Pt 2):661–9. doi: 10.1042/bj20021287

40. Dikalov S, Griendling KK, Harrison DG. Measurement of reactive oxygen species in cardiovascular studies. *Hypertension* (2007) 49(4):717–27. doi: 10.1161/01.HYP.0000258594.87211.6b

41. Chakrabarti S, Visweswariah SS. Intramacrophage ROS primes the innate immune system *via* JAK/STAT and toll activation. *Cell Rep* (2020) 33(6):108368. doi: 10.1016/j.celrep.2020.108368

42. Kondo S, Takahashi T, Yamagata N, Imanishi Y, Katow H, Hiramatsu S, et al. Neurochemical organization of the drosophila brain visualized by endogenously tagged neurotransmitter receptors. *Cell Rep* (2020) 30(1):284–97 e5. doi: 10.1016/j.celrep.2019.12.018

43. Diao F, White BH. A novel approach for directing transgene expression in Drosophila: T2A-Gal4 in-frame fusion. *Genetics* (2012) 190(3):1139–44. doi: 10.1534/genetics.111.136291

44. Gyoergy A, Roblek M, Ratheesh A, Valoskova K, Belyaeva V, Wachner S, et al. Tools allowing independent visualization and genetic manipulation of drosophila melanogaster macrophages and surrounding tissues. *G3 (Bethesda)* (2018) 8(3):845–57. doi: 10.1534/g3.117.300452

45. Chintapalli VR, Wang J, Dow JA. Using FlyAtlas to identify better Drosophila melanogaster models of human disease. *Nat Genet* (2007) 39(6):715–20. doi: 10.1038/ng2049

46. Korona D, Dirnberger B, Giachello CNG, Queiroz RML, Minde D-P, Deery MJ, et al. Drosophila nicotinic acetylcholine receptor subunits and their native interactions with insecticidal peptide toxins. *bioRxiv* (2021). 2021.08.13.456240. doi: 10.1101/2021.08.13.456240

47. Honti V, Csordas G, Markus R, Kurucz E, Jankovics F, Ando I. Cell lineage tracing reveals the plasticity of the hemocyte lineages and of the hematopoietic compartments in Drosophila melanogaster. *Mol Immunol* (2010) 47(11-12):1997–2004. doi: 10.1016/j.molimm.2010.04.017

48. Zirin J, Hu Y, Liu L, Yang-Zhou D, Colbeth R, Yan D, et al. Large-scale transgenic drosophila resource collections for loss- and gain-of-function studies. *Genetics* (2020) 214(4):755–67. doi: 10.1534/genetics.119.302964

49. Watson GB, Chouinard SW, Cook KR, Geng C, Gifford JM, Gustafson GD, et al. A spinosyn-sensitive Drosophila melanogaster nicotinic acetylcholine receptor

identified through chemically induced target site resistance, resistance gene identification, and heterologous expression. *Insect Biochem Mol Biol* (2010) 40 (5):376–84. doi: 10.1016/j.ibmb.2009.11.004

50. Shin M, Cha N, Koranteng F, Cho B, Shim J. Subpopulation of macrophage-like plasmatocytes attenuates systemic growth *via* JAK/STAT in the drosophila fat body. *Front Immunol* (2020) 11:63. doi: 10.3389/fimmu.2020.00063

51. Stramer B, Wood W, Galko MJ, Redd MJ, Jacinto A, Parkhurst SM, et al. Live imaging of wound inflammation in Drosophila embryos reveals key roles for small GTPases during in *vivo* cell migration. *J Cell Biol* (2005) 168(4):567–73. doi: 10.1083/jcb.200405120

52. Sinenko SA, Mathey-Prevot B. Increased expression of Drosophila tetraspanin, Tsp68C, suppresses the abnormal proliferation of ytr-deficient and Ras/Raf-activated hemocytes. *Oncogene* (2004) 23(56):9120–8. doi: 10.1038/sj.onc.1208156

53. Perez-Cadahia B, Drobic B, Davie JR. H3 phosphorylation: dual role in mitosis and interphase. *Biochem Cell Biol* (2009) 87(5):695–709. doi: 10.1139/O09-053

54. Song Z, McCall K, Steller H. DCP-1, a Drosophila cell death protease essential for development. *Science* (1997) 275(5299):536–40. doi: 10.1126/science.275.5299.536

55. Rotelli MD, Bolling AM, Killion AW, Weinberg AJ, Dixon MJ, Calvi BR. An RNAi screen for genes required for growth of drosophila wing tissue. *G3 (Bethesda)* (2019) 9(10):3087–100. doi: 10.1534/g3.119.400581

56. Salvaterra PM, Kitamoto T. Drosophila cholinergic neurons and processes visualized with Gal4/UAS-GFP. *Brain Res Gene Expr Patterns* (2001) 1(1):73–82. doi: 10.1016/S1567-133X(01)00011-4

57. Sanyal S. Genomic mapping and expression patterns of C380, OK6 and D42 enhancer trap lines in the larval nervous system of Drosophila. *Gene Expr Patterns* (2009) 9(5):371–80. doi: 10.1016/j.gep.2009.01.002

58. Johansen J, Halpern ME, Johansen KM, Keshishian H. Stereotypic morphology of glutamatergic synapses on identified muscle cells of Drosophila larvae. *J Neurosci* (1989) 9(2):710–25. doi: 10.1523/JNEUROSCI.09-02-00710.1989

59. Lacin H, Chen HM, Long X, Singer RH, Lee T, Truman JW. Neurotransmitter identity is acquired in a lineage-restricted manner in the Drosophila CNS. *Elife* (2019) 8. doi: 10.7554/eLife.43701

60. Makhijani K, Alexander B, Rao D, Petraki S, Herboso L, Kukar K, et al. Regulation of Drosophila hematopoietic sites by Activin-beta from active sensory neurons. *Nat Commun* (2017) 8:15990. doi: 10.1038/ncomms15990

61. Cheng LE, Song W, Looger LL, Jan LY, Jan YN. The role of the TRP channel NompC in Drosophila larval and adult locomotion. *Neuron* (2010) 67(3):373–80. doi: 10.1016/j.neuron.2010.07.004

62. Song W, Onishi M, Jan LY, Jan YN. Peripheral multidendritic sensory neurons are necessary for rhythmic locomotion behavior in Drosophila larvae. *Proc Natl Acad Sci U S A* (2007) 104(12):5199–204. doi: 10.1073/pnas.0700895104

63. Hughes CL, Thomas JB. A sensory feedback circuit coordinates muscle activity in Drosophila. *Mol Cell Neurosci* (2007) 35(2):383–96. doi: 10.1016/j.mcn.2007.04.001

64. Hwang RY, Zhong L, Xu Y, Johnson T, Zhang F, Deisseroth K, et al. Nociceptive neurons protect Drosophila larvae from parasitoid wasps. *Curr Biol* (2007) 17 (24):2105–16. doi: 10.1016/j.cub.2007.11.029

65. Lagueux M, Perrodou E, Levashina EA, Capovilla M, Hoffmann JA. Constitutive expression of a complement-like protein in toll and JAK gain-of-function mutants of Drosophila. *Proc Natl Acad Sci U S A* (2000) 97(21):11427–32. doi: 10.1073/pnas.97.21.11427

66. Dostalova A, Rommelaere S, Poidevin M, Lemaitre B. Thioester-containing proteins regulate the Toll pathway and play a role in Drosophila defence against microbial pathogens and parasitoid wasps. *BMC Biol* (2017) 15(1):79. doi: 10.1186/s12915-017-0408-0

67. Irving P, Ubeda JM, Doucet D, Troxler L, Lagueux M, Zachary D, et al. New insights into Drosophila larval haemocyte functions through genome-wide analysis. *Cell Microbiol* (2005) 7(3):335–50. doi: 10.1111/j.1462-5822.2004.00462.x

68. Evans CJ, Liu T, Girard JR, Banerjee U. Injury-induced inflammatory signaling and hematopoiesis in Drosophila. *bioRxiv* (2021). 2021.10.13.464248. doi: 10.1101/2021.10.13.464248

69. Baeg GH, Zhou R, Perrimon N. Genome-wide RNAi analysis of JAK/STAT signaling components in Drosophila. *Genes Dev* (2005) 19(16):1861–70. doi: 10.1101/gad.1320705

70. Ramond E, Jamet A, Ding X, Euphrasie D, Bouvier C, Lallemant L, et al. Reactive oxygen species-dependent innate immune mechanisms control methicillin-resistant staphylococcus aureus virulence in the drosophila larval model. *mBio* (2021) 12(3): e0027621. doi: 10.1128/mBio.00276-21

71. Li Z, Wu C, Ding X, Li W, Xue L. Toll signaling promotes JNK-dependent apoptosis in Drosophila. *Cell Div* (2020) 15:7. doi: 10.1186/s13008-020-00062-5

72. Hodo TW, de Aquino MTP, Shimamoto A, Shanker A. Critical neurotransmitters in the neuroimmune network. *Front Immunol* (2020) 11:1869. doi: 10.3389/fimmu.2020.01869

73. Madhwal S, Shin M, Kapoor A, Goyal M, Joshi MK, Ur Rehman PM, et al. Metabolic control of cellular immune-competency by odors in Drosophila. *Elife* (2020) 9. doi: 10.7554/eLife.60376

74. Qi YX, Huang J, Li MQ, Wu YS, Xia RY, Ye GY. Serotonin modulates insect hemocyte phagocytosis via two different serotonin receptors. *Elife* (2016) 5. doi: 10.7554/eLife.12241

75. Kapoor A, Padmavathi A, Mukherjee T. Dual control exerted by dopamine in blood-progenitor cell cycle regulation in Drosophila. *bioRxiv* (2021). 2021.03.29.437463. doi: 10.1101/2021.03.29.437463

76. Dupuis J, Louis T, Gauthier M, Raymond V. Insights from honeybee (Apis mellifera) and fly (Drosophila melanogaster) nicotinic acetylcholine receptors: from genes to behavioral functions. *Neurosci Biobehav Rev* (2012) 36(6):1553–64. doi: 10.1016/j.neubiorev.2012.04.003

77. Rosenthal JS, Yuan Q. Constructing and tuning excitatory cholinergic synapses: the multifaceted functions of nicotinic acetylcholine receptors in drosophila neural development and physiology. *Front Cell Neurosci* (2021) 15:720560. doi: 10.3389/fncel.2021.720560

78. Giordani G, Cattabriga G, Becchimanzi A, Di Lelio I, De Leva G, Gigliotti S, et al. Role of neuronal and non-neuronal acetylcholine signaling in Drosophila humoral immunity. *Insect Biochem Mol Biol* (2023) 153:103899. doi: 10.1016/j.ibmb.2022.103899